

3D near-surface velocity model building by joint seismic-airborne EM inversion

Guy Marquis*, Shell International Exploration & Production Company Inc., Weizhong Wang and Jide Ogunbo, GeoTomo LLC

Summary

We propose here a methodology to build near-surface velocity models by joint inversion of traveltime and high-resolution airborne EM (AEM) data. The resulting velocity and resistivity models are steered to be structurally similar through the inclusion of a cross-gradient term in the objective function. The inversion is stable and results in better-fitting velocity and resistivity models. The resulting velocity model is then used to compute statics corrections on pre-stack seismic data. We tested the method on high-quality coincident 3D seismic and AEM data from Canada by computing three different near-surface velocity models: Model 1 is a traveltime tomography using the first breaks of all the seismic shots and receivers, Models 2 and 3 are a traveltime tomography and a joint seismic-AEM inversion with a limited number of shots. The resulting stacks using statics corrections from Models 1 and 3 are very similar but the stack using Model 2 is not as sharp as the others. Our results suggest that adding AEM data to a seismic dataset with fewer shots produces seismic images as good as when a large number of shots are included.

Introduction

Accounting for near-surface heterogeneities is an important problem when processing land seismic data. Such heterogeneities can be due to rugged topography, sharp lateral velocity contrasts or low-velocity layers. Different methods have been introduced to address these statics problems such as generalized linear inversion, first-arrival traveltime tomography, refraction traveltime migration or surface-wave dispersion curve inversion, which generally give good results. However the seismic data acquisition topologies are usually optimized to image deep targets and so are often inappropriate for near-surface characterization.

Several authors have recently tried to get around this problem by combining seismic data with data from other geophysical methods focused on the near-surface. Colombo and Keho (2010) performed structurally constrained joint non-seismic and seismic inversion to solve near-surface problems in Saudi Arabia. Colombo et al. (2012, 2015) enforced structural constraints to perform joint inversion of high-resolution EM, gravity and seismic datasets. Pineda et al. (2015) used electrical and EM data to improve up-hole velocity models.

In this study, we propose a novel methodology for joint inversion of data sets from seismic and time- or frequency-

domain airborne EM (AEM) data applied to 3D datasets. A first example of a 2D application was presented by Marquis et al. (2016).

Joint seismic-AEM inversion

The subsurface can be characterized by, among other properties, seismic velocity and electrical resistivity. Although these properties may not have a direct physical relationship between them, their subsurface variations might be coincident (e.g. Gallardo and Meju, 2011). One way to impose structural similarity is to use their cross-gradient which depends on the direction of the property variations rather than on their magnitude.

Defining the cross-gradient t as a structural constraint (e.g. Gallardo and Meju, 2003, 2004), the joint inversion's objective function \emptyset becomes:

$$\begin{aligned} \emptyset(m_e, m_s) = & \xi_e (\|\mathbf{W}_e(d_e - G_e(m_e))\|^2 + \tau_e \|\mathbf{L}m_e\|^2) \\ & + \xi_s (\|\mathbf{W}_s(d_s - G_s(m_s))\|^2 + \tau_s \|\mathbf{L}m_s\|^2) \\ & + \lambda \|t\|^2 \end{aligned} \quad (1)$$

where the parameters with subscripts e and s correspond to AEM and seismic terms respectively; m 's are the subsurface models, ξ 's are the misfit scaling factors, d 's are the observed data, $G(m)$ are the model responses, \mathbf{W} 's are the data weights, \mathbf{L} is a regularization operator, τ 's are the regularization weights and λ is the cross-gradient weight. The cross-gradient term t is given as (Gallardo and Meju, 2003, 2004):

$$t(\log(m_e), m_s) = \nabla \log(m_e(x, z)) \times \nabla m_s(x, z). \quad (2)$$

We point out that minimizing the cross-gradient results in increasing the structural similarity between the two models.

Note that equation (1) does not require the models to follow any a-priori petrophysical relationship. While it might be beneficial to include this information in the inversion process, we have decided to ignore it and focus on maximizing the structural similarities.

Application to 3D data

We apply our new methodology to coincident seismic and AEM surveys acquired for Shell Canada. The seismic data have been acquired with EM shot lines and NS receiver lines with shot and receiver interval both at 50 m.

Joint seismic-airborne EM inversion

The AEM data used here have been acquired with a Fugro (now CGG) Airborne RESOLVE system, and consist of the real and imaginary parts of the secondary-to-primary field ratio at five frequencies. Line spacing was 100 m and the instrument was flown on average 35 m above the earth surface.

We produced three different 3D near-surface velocity models using the following workflow:

- Compute a traveltime tomography model that includes all (3542) shots and all receivers. This will be Model 1, our benchmark velocity model.
- Decimate the shot space by keeping only one shot per square km (68 shots) and all receivers, as a means to assess the benefit of adding tightly-sampled AEM data to a sparsely-sampled seismic data set.
- Starting from a homogeneous half-space, invert separately the decimated seismic (resulting in Model 2) and AEM data to bring both models close to their optimal solution. Both inversions converged rapidly.
- Use the two models found above as starting models for the joint inversion and start applying the cross-

gradient constraint at the second iteration. The resulting model is Model 3.

For the example shown below, we have put strong weights on the seismic data misfit and on the cross-gradient (ξ_s and λ in equation 1 above), while we have kept the weight of the AEM data misfit (ξ_e) at zero.

We can visualize the convergence of the joint inversion by looking at the evolution of the AEM data misfit, traveltime data misfit and cross-gradient (Figure 1). The AEM misfit remains stable from the second iteration and the traveltime misfit increases slightly from that of its standalone inversion and then gradually decreases to a much lower value. The cross-gradient decreases rapidly up to iteration 5, then oscillates near its minimum, indicating that the velocity and resistivity models have become more similar. We conclude from these observations that the joint inversion is indeed able to make the two models more similar, essentially improving the velocity model; the resistivity model undergoes marginal changes throughout the joint inversion process.

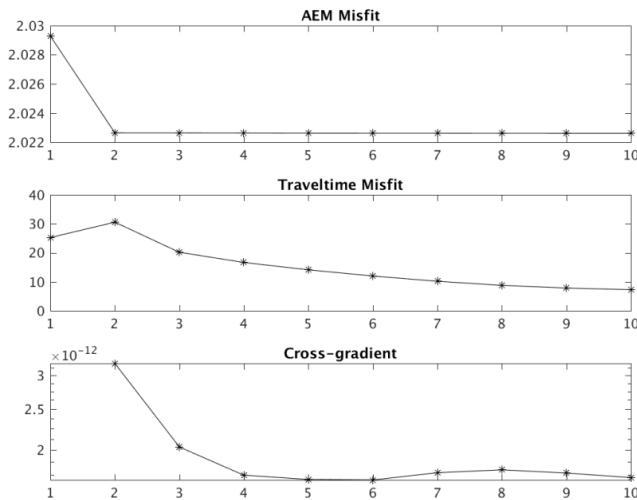


Figure 1. Airborne EM (top) and seismic traveltime (center) misfits and cross-gradient (bottom) as a function of iteration number for the joint seismic-AEM inversion. The cross-gradient is applied from the second iteration.

Depth slices from the resulting models from the different standalone and joint inversions are presented in Figure 2. The effect of shot decimation is clear when comparing Models 1 (top left) and 2 (top right): ray-path artifacts produce spotty velocity anomalies in the vicinity of the selected shots. The slice from Model 3 (bottom left) shows

clearly the benefit of adding high-resolution, dense AEM data into the joint inversion: ray-path artifacts are removed, shorter wavelength features are introduced and the resulting model shares features with Model 1. For sake of comparison, we show the joint inversion resistivity model (bottom right) that has structural features similar to Model

Joint seismic-airborne EM inversion

3, a consequence of applying the cross-gradient. These results clearly show that joint inversion produces a far better near-surface velocity model.

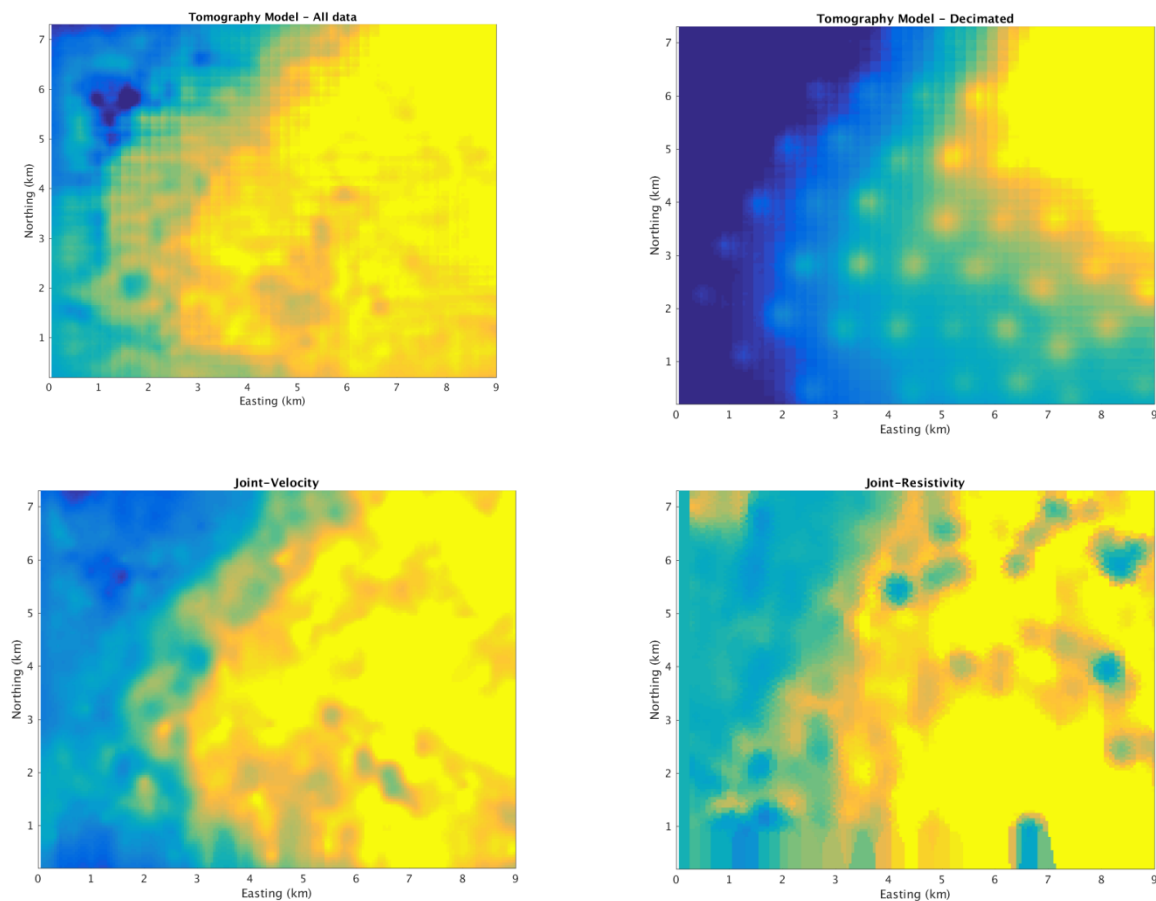


Figure 2. Depth slice (800 m a.s.l.) of the velocity model from travel-time tomography of all (Model 1, top left) and decimated (Model 2, top right) seismic data and from velocity (Model 3, bottom left) and resistivity (bottom right) models from joint seismic-AEM inversion.

The near-surface velocity models obtained by traveltimes tomography and joint seismic-AEM inversion are used to compute their respective static corrections. We extracted 2D lines from the original data and processed them with the same standard sequence (except for statics) to produce stack sections, excerpts of which are shown in Figure 3 below. We compare here three stacks using statics computed from Models 1, 2 and 3. Here again, the stack from Model 1 is used as a benchmark.

The stacks using statics from Models 1 (left) and 3 (center) are very similar and are both much sharper than the stack using statics from Model 2 (right). Shallow (< 1.1 s twt) reflector continuity is arguably better with Model 1 but from 1.1 twt and beyond, stacked sections 1 and 3 are essentially the same. By comparison, the stack using Model 2 statics shows poorer reflector continuity and some undulations on reflectors that are flat in the other two sections.

Joint seismic-airborne EM inversion

Conclusion

We developed a joint seismic-airborne EM inversion methodology and computed 3D near-surface velocity models. These first 3D results illustrate how the integration of high-resolution AEM data can improve near-surface velocity models - and hence seismic images - in situations where the shot coverage is sparse.

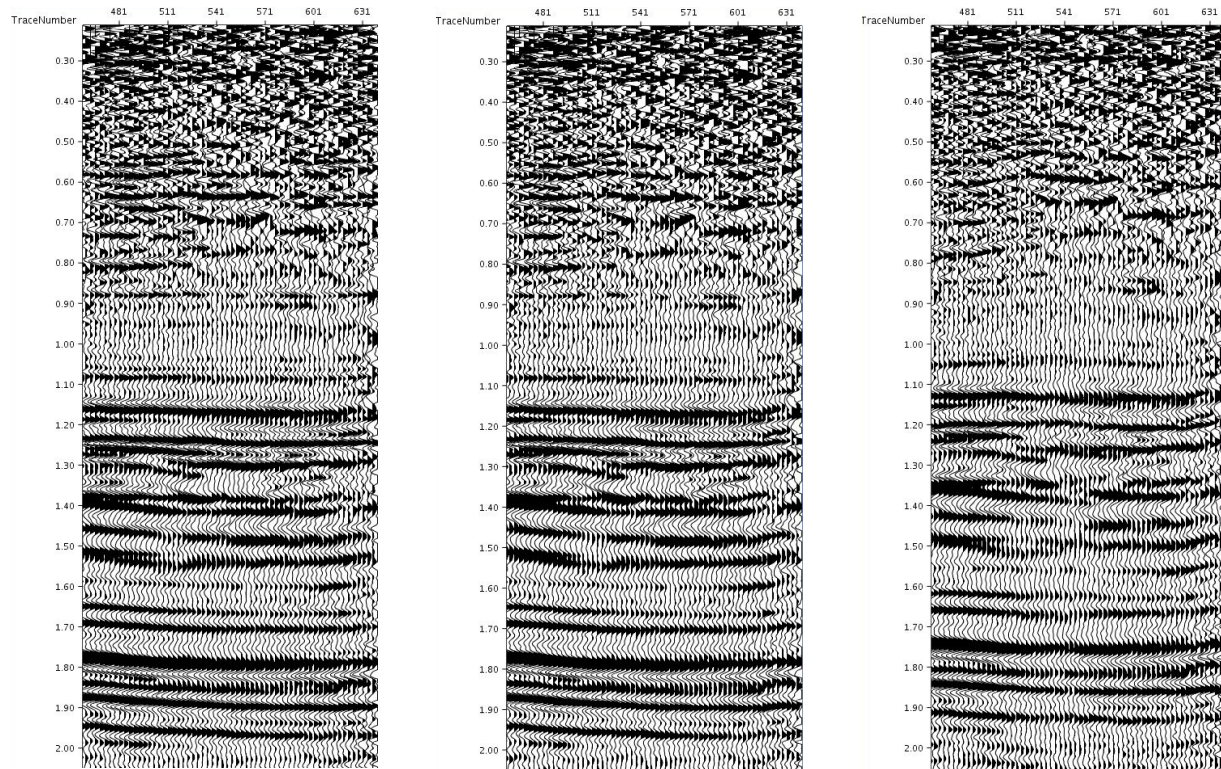


Figure 3. Excerpts from stack sections with statics computed using standalone traveltimes tomography on all shots (Model 1, left), joint seismic-AEM inversion (model 3, center) and traveltimes tomography on selected shots (Model 2, right).

Acknowledgments

We thank Shell Canada Limited for allowing us to present their data.

EDITED REFERENCES

Note: This reference list is a copyedited version of the reference list submitted by the author. Reference lists for the 2016 SEG Technical Program Expanded Abstracts have been copyedited so that references provided with the online metadata for each paper will achieve a high degree of linking to cited sources that appear on the Web.

REFERENCES

- Colombo, D., and T. Keho, 2010, The non-seismic data and joint inversion strategy for the near surface solution in Saudi Arabia: 80th Annual International Meeting, SEG, Expanded Abstracts, 1934–1938, <http://dx.doi.org/10.1190/1.3513222>.
- Colombo, D., G. McNeice, and R. Ley, 2012, Multigeophysics joint inversion for complex land seismic imaging in Saudi Arabia: 82nd Annual International Meeting, SEG, Expanded Abstracts, 1–5. <http://dx.doi.org/10.1190/segam2012-0441.1>.
- Colombo, D., G. McNeice, D. Rovetta, E. Turkoglu, A. Sena, E. Sandoval-Curiel, F. Miorelli, and Y. Taqi, 2015, Super resolution multi-geophysics imaging of a complex wadi for near surface corrections: 85th Annual International Meeting, SEG, Expanded Abstracts, 849–853, <http://dx.doi.org/10.1190/segam2015-5841055.1>.
- Gallardo, L. A., and M. A. Meju, 2003, Characterization of heterogeneous near-surface materials by joint 2D inversion of dc resistivity and seismic data: *Geophysical Research Letters*, **30**, 1658, <http://dx.doi.org/10.1029/2003GL017370>.
- Gallardo, L. A., and M. A. Meju, 2004, Joint two-dimensional DC resistivity and seismic travel time inversion with cross-gradients constraints: *Journal of Geophysical Research*, **109**, B03311, <http://dx.doi.org/10.1029/2003JB002716>.
- Gallardo, L. A., and M. A. Meju, 2011, Structure-coupled multiphysics imaging in geophysical sciences: *Reviews of Geophysics*, **49**, RG1003, <http://dx.doi.org/10.1029/2010RG000330>.
- Marquis, G., W. Wang, J. Ogunbo, and D. Mu, 2016, Joint seismic-airborne EM inversion for near-surface velocity model building: GeoConvention.
- Pineda, A., S. Gallo, and H. Harkas, 2015, Geophysical near-surface characterization for static corrections: Multi-physics survey in Reggane Field, Algeria: 77th Annual International Conference and Exhibition, EAGE, Expanded Abstracts, <http://dx.doi.org/10.3997/2214-4609.201412990>.